

Research Article

Synthesis and Characterization of Ce-Doped $Y_3Al_5O_{12}$ (YAG:Ce) Nanopowders Used for Solid-State Lighting

Do Ngoc Chung,¹ Do Ngoc Hieu,¹ Tran Thi Thao,¹
Vo-Van Truong,² and Nguyen Nang Dinh¹

¹ University of Engineering and Technology, Vietnam National University, Hanoi, 144 Xuan Thuy Road, Cau Giay District, Hanoi 10000, Vietnam

² Department of Physics, Concordia University, 1455 de Maisonneuve Boulevard W, Montreal, QC, Canada H3G 1M8

Correspondence should be addressed to Nguyen Nang Dinh; dinh158@yahoo.com

Received 10 December 2013; Revised 5 May 2014; Accepted 6 May 2014; Published 25 May 2014

Academic Editor: Prashant Kumar

Copyright © 2014 Do Ngoc Chung et al. This is an open access article distributed under the Creative Commons Attribution License, which permits unrestricted use, distribution, and reproduction in any medium, provided the original work is properly cited.

Nano-Ce-doped $Y_3Al_5O_{12}$ (YAG:Ce) powders were synthesized by using a sol-gel low temperature combustion method, followed by thermal annealing. The annealing temperature for enriching nanoparticles was optimized and found to be 1000°C. The process for enriching uniform nanoparticles of YAG:Ce powder was carried out by using the nanosteam technique (NST). The nanoparticles obtained from this NST treatment had a size in the range of 9–20 nm. Measurements of the photoluminescence spectra of the dispersed YAG:Ce nanoparticles solutions showed a blue shift in the photoemission with a value of ca. 10 nm in the green region. WLEDs made from the blue LED chip coated with the nano-YAG:Ce + MEH-PPV composite epoxy exhibit white light with a broad band luminescent spectrum and a high color rendering index (CRI). The photoluminescence spectra of the YAG:Ce nanoparticles showed a potential application of the prepared nanostructured YAG:Ce phosphor not only in energy-efficient solid-state lighting, but also in optoelectronic devices, including organic composite solar cells. In addition, it is suggested that NST can be applied for the enrichment of uniform inorganic nanoparticles.

1. Introduction

Research and applications of solid-state lighting (SSL) have grown exponentially in the world since the discovery of InGaN fabrication process by Nakamura et al. [1]. The rapid development of white light-emitting diodes (WLED) over the last few years has opened new opportunities in the general illumination market [2, 3]. Moreover, the SSL consumes less electricity and does not cause much pollution, the development of the SSL devices can be seen as a valuable contribution in the maintenance of environment. The efficiency of commercialized WLEDs is now around 80 lm/W, which is comparable with that of fluorescent lamps. There are several approaches to fabricate white LED, for instance, by using a blue or UV LED to excite some phosphors to give white light [4]. The ability to obtain different color correlated temperature (CCT) and high color rendering index (CRI) of WLED gives new features to this kind of light sources.

It is known that $Y_3Al_5O_{12}$ - (YAG-) based materials are commonly used as a host material in various solid-state lasers. Rare earth elements such as neodymium and erbium can be doped into YAG as active laser ions, yielding YAG:Nd and YAG:Er lasers, respectively. Recently, YAGs have also been developed for energy-efficient SSL [5]. For this, Ce is doped in YAG (YAG:Ce) and this material is used to cover the InGaN-LED chips to get white light from WLED. Under blue light excitation of the LED chips, YAG:Ce phosphor emits a broad spectrum from 500 to 650 nm, due to the 5d-4f transition of Ce^{3+} ion [6]. This is the reason why YAG:Ce phosphor has extensive application in WLEDs.

There are many methods used for the preparation of the YAG powder with a high crystallinity, a large luminous power, and a small particle size, such as methods using solid-state reaction [7–10], coprecipitation, [11–13] and sol-gel process [14]. As Yan et al. reported in [15], YAG:Ce with nanoparticles may be prepared by a sol-gel low temperature combustion

method (shortly called LTC). Recently, we have also synthesized YAG:Ce by this method. However, the LTC-synthesized YAG:Ce powder product usually contained particles with a size ranging from a few to hundreds of nanometers. With the aim of preparing a solution of nano-YAG:Ce particles one can use a traditional technique, the so-called “water dispersion technique” (WDT) using either ultrasonic or magnetic stirring. This method is simple; however, it will be seen in Section 3 that the WDT-dispersion solution exhibits an incomplete separation of nanoparticles from the larger size particles.

The size and shape of powders influence the flow and compaction properties. Larger, more spherical particles will typically flow more easily than smaller or high aspect ratio particles. Smaller particles dissolve more quickly and lead to higher suspension viscosities than larger ones. In order to measure the particles size with the LB550 machine, it is necessary to dissolve the YAG:Ce powder in a solution. However, when the YAG:Ce powder is dispersed in a solution, particles usually cluster in aggregates. This results in a large error in the determined size of the particles. The size measured by LBP550 is much larger than the real particle size. That is true because when the YAG:Ce powder is dispersed in solution or air, the nanoparticles will coalesce due the effect of nanoparticle interactions. The coalescence of nanoparticles leads to reducing potential of particles, as reported elsewhere [16].

With the aim of producing nano-YAG:Ce phosphor powder, a dispersion solution with uniform nanoparticles of the YAG:Ce was prepared by using a nanosteam technique (NST). In this work, we present the results on the process of the nanoparticles enrichment from the LTC-prepared YAG:Ce powder and characterization of the size distribution of nanoparticles by using a dynamic light scattering particle size analyzer combined with the NST treatment. Finally, the nano-YAG:Ce powder was used with a conjugate polymer Poly[2-methoxy-5-(2'-ethyl-hexyloxy)-1,4-phenylene vinylene] (MEH-PPV) to prepare the nanocomposite coating for WLEDs as solid-state lighting (SSL).

The crystalline structure, surface morphology, and photoluminescent properties of YAG:Ce powders and emission spectra of the WLEDs were also studied.

2. Experimental

2.1. Preparation of the YAG:Ce Phosphor Powder. Nanocrystalline YAG and YAG:Ce (with a Ce concentration of 2 wt%) powders were prepared by the LTC method, following the process as reported elsewhere [15, 17]. High purity chemicals were used: Y_2O_3 , HNO_3 , $Ce(NO_3)_3 \cdot 6H_2O$, $Al(NO_3)_3 \cdot 9H_2O$, $C_6H_8O_7 \cdot H_2O$, and ammonia ($NH_3 \cdot H_2O$).

The YAG:Ce powder with a composition corresponding to the chemical stoichiometry formula of $Y_3Al_5O_{12}:Ce$ was synthesized from the above mentioned precursor materials. Y_2O_3 was dissolved in a hot nitric acid in a three-neck flask and prepared solution. The solution was agitated for 2 hours at temperature of $60^\circ C$ – $65^\circ C$ in nitrogen gas. Then the solution was added with aluminum nitrate and cerium

nitrate to get the bright yellow solution. In the next step, citric acid ($C_6H_8O_7 \cdot H_2O$) was added in the bright yellow solution. Citric acid was dissolved in this solution by half the mole of the total metal ions. The pH value of the solution was modulated to 8, and a gel was obtained in 60 min by immersing the solution in a water bath at $80^\circ C$. Then the gels were dried to obtain canary xerogel. The xerogel was put into a muffle stove and a combustion reaction occurred at $245^\circ C$ for 20 min, and the spumous powder was obtained. The calcination was conducted at $700^\circ C$ with a heating rate of $2^\circ C/min$ and kept for 300 min; then, the temperature was increased to different holding temperatures (800 , 1000 , and $1200^\circ C$) at a rate of $10^\circ C/min$ for a fixed holding time of 120 min in nitrogen gas.

2.2. Set-Up of the Nanosteam Technique System. In order to enrich YAG-Ce nanoparticles in a water solution as well as to improve the precision of the measurement of the particle size on the LB-550 machine, we set up a system using the NST method as shown in the following diagram (Figure 1).

The YAG:Ce powder was put in air column pots at the bottom. Clean air is blown in the air column pot, making the YAG:Ce nanopowder separated from the powder form in steam. The steam will move in to water pots by pump. After a certain period, the solution taken from the water pot (3) was used for the particle size distribution measurements on the LB550 machine. In this system, both the height of air column pots and the pumping pressure play an important role; they affect the particles' separation of the powder that is obtained in the solution pot (3). From our experiments, the optimum parameters of the air column height and the pressure for the NST process were found to be of 30 cm and 250 mbar, respectively. Nanopowder of YAG:Ce was then collected from the column and reannealed at $450^\circ C$ for 2 h. This powder was further used for characterization and preparation of nanocomposites that were coated onto a blue LED chip to get the solid-state lighting lamp.

To compare the NST with the WDT method regarding particles dispersion, we also dispersed 5 g of the YAG:Ce powders in a 100 mL capacity glass with 80 mL of distilled water by using both the ultrasonic and magnetic stirring. The time for each stirring lasted for over 10 h. The dispersion solution was left to be immovable for 5 hours; then, 30 mL from the top of the dispersion solution level was taken for further measurements.

We used dynamic light scattering technique for the determination of the particle size of YAG:Ce powder. The DLS is based on the Brownian motion of particles and the Doppler effect [18]; it can be applied to determine the particle size distribution over a range from 1 nm to $6 \mu m$. A sample particle (or droplet), exposed to laser light, diffuses light with a changed frequency. This frequency change compared to the original light varies directly with the velocity of moving particles. By analyzing the frequency change, one can obtain the distribution of the particle size of samples. A “HORIBA-LB550” instrument offers the possibility to control these parameters in real time. The viscosity issue becomes even more critical as the analyzed sample concentration is increased.

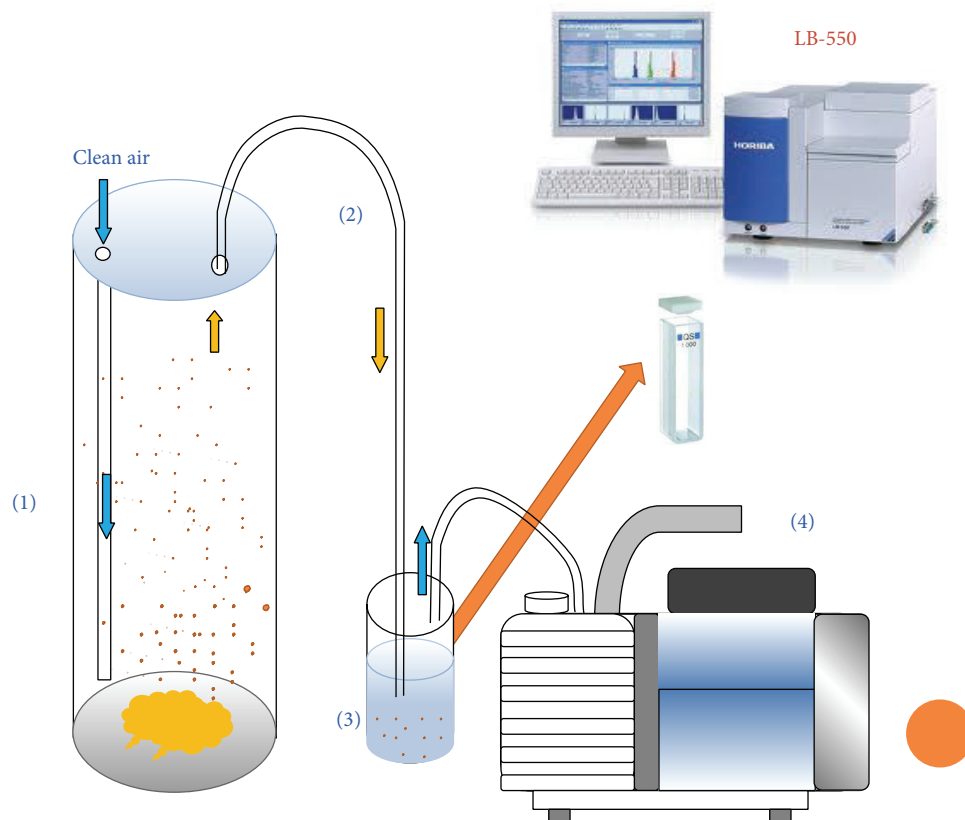


FIGURE 1: Schematic diagram for measuring YAG:Ce nanoparticle size by LB-550 with nanosteam technique: air column pots (1), gas pipe (2), water pots (3), and vacuum pump (4).

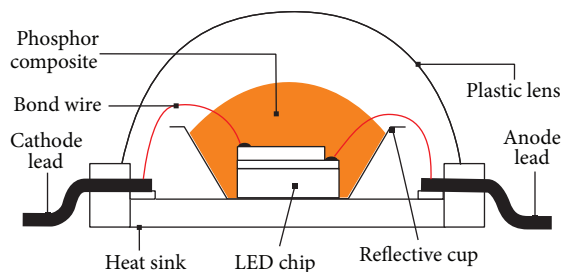


FIGURE 2: Scheme of a WLED made from a composite of nano-YAG:Ce and conjugate polymer MEH-PPV (YAG:Ce + MEH-PPV). The average thickness of the phosphor composite layer is $\sim 700 \mu\text{m}$.

2.3. Preparation of WLED for Solid-State Lighting. To prepare nanocomposite, the YAG:Ce nanopowder was mixed with the MEH-PPV according to a volume ratio of 10 : 1. For this, the pure MEH-PPV solution was prepared by dissolving the MEH-PPV powder in toluene solvent with a ratio of 1 mg of MEH-PPV powder in 2 mL toluene. The nano-YAG:Ce powder in the MEH-PPV solution was mixed in a liquid transparent epoxy. The obtained composite epoxy was then coated onto the blue LED chip, followed by annealing at 150°C to get WLED, as shown in Figure 2. For the investigation of spectroscopic properties, some samples were made by

coating YAG:Ce + MEH-PPV solution onto glass or quartz substrates.

2.4. Characterization Techniques. X-ray diffraction (XRD) was used for analyzing the crystalline phases in the samples. The XRD patterns were obtained from a Bruker X-ray diffractometer “D8 Advance.” The morphology characterization of the samples was carried out on a Hitachi scanning electron microscope “S4800-NIHE” (FE-SEM). The distribution of the size of YAG:Ce particles was analyzed by using a HORIBA dynamic light scattering particle size analyzer “LB-550.” The absorption and photoluminescent spectra of the composite films were recorded on JASCO “UV/VIS/NIR spectrophotometer V-570” and a HORIBA high resolution FLuoroMax-4 spectrofluorometer “Microspec-235b,” respectively. The electroluminescence characterizations were measured by using an integrating sphere equipped with a calibrated spectrophotometer-“LCS 100” (LED measurement System).

The blue InGaN-LED chip used in this research is the high power 1 W LED chip with the emission peak at 455 nm (with the die size around $1100 \mu\text{m} \times 1100 \mu\text{m}$, as can be seen elsewhere [12]). The green YAG:ce phosphor and MEH-PPV polymer hybrid composite were dropped onto the surface area between the top of the LED chip to convert a part of blue light into green and red lights.

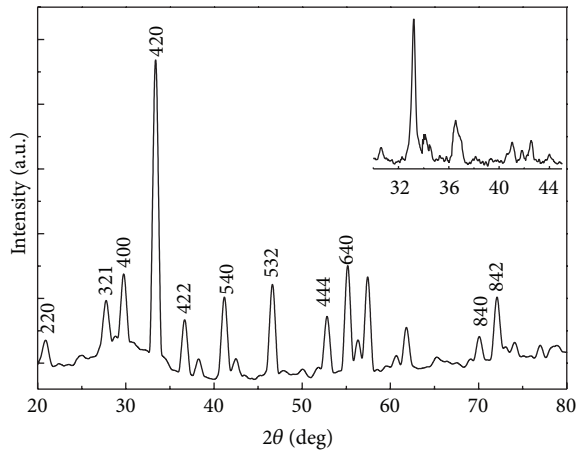


FIGURE 3: XRD patterns of samples at 1000°C annealing temperatures. The insertion is XRD of the collected nanopowder.

3. Results and Discussion

3.1. Crystalline Structures and Photoluminescent Property. The XRD patterns of a typical YAG:Ce prepared by the LTC method are shown in Figure 3. All the peaks revealed in the patterns are consistent with the characteristic peaks of the bulk YAG crystal (pdf card no. 12005-21-9). In the insertion, a part of the XRD patterns (viz., the peaks of the (420), (422), and (540) diffraction crystalline planes) for the nanopowder collected from the water pot is shown. The XRD patterns indicate a well-crystallized YAG sample. The Ce-doping did not affect the crystalline structure, showing the substitution doping of Ce atoms in the YAG lattice. The CeO₂ phase did not appear in the XRD patterns. For as-prepared YAG:Ce samples, the fact that all the XRD peaks are strong and sharp proves that the majority of the sample volume contains macrocrystallites.

After the NST treatment, the collected powder from the YAG volume exhibits nanostructured characteristics. This is confirmed by the fact that the XRD peak width became much larger. To determine the particle size (τ), we used Scherrer's formula [19]:

$$\tau = \frac{0.9\lambda}{\beta \cdot \cos \theta}, \quad (1)$$

where λ is the X-ray wavelength used, β is the full width at half maximum in radians, and θ is the Bragg angle of the considered diffraction peak. The average value of the particles calculated from XRD peaks was found to be 20 nm.

Emission intensity is one of the key parameters for the application of the YAG:Ce powder. Figure 3 shows a typical PL spectrum of the YAG:Ce powder prepared by the LTC method at an annealing temperature of 1200°C and a Ce concentration of 2 wt%. The PL curve in Figure 4 shows the characteristic $4f \rightarrow 5d$ transitions of Ce³⁺ in YAG:Ce crystals under excitation in the blue region around 442 nm. The PL spectrum of the YAG:Ce powder exhibits a broad maximum in the green region centered at 520 nm. This is one of the

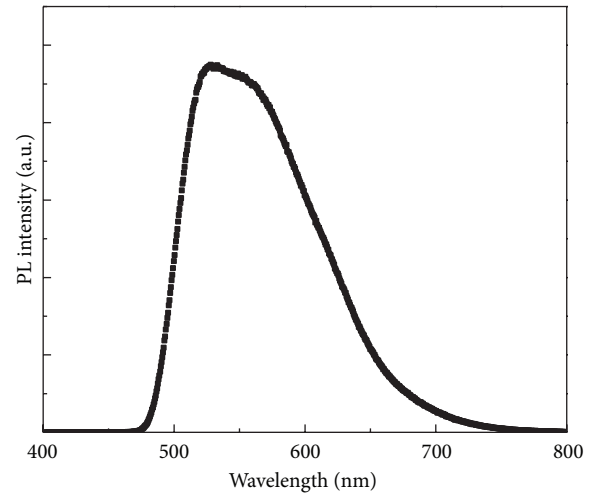


FIGURE 4: Photoluminescence of YAG:Ce at 442 nm excitation wavelength.

desired properties of the YAG phosphor that can be used for energy-efficient solid-state lighting.

3.2. Nanosize Properties of YAG:Ce. Figure 5 shows the FE-SEM images of YAG:Ce powder annealed at low temperature (700°C), middle temperature (1000°C), and high temperature (1200°C). From this figure one can see that the particle size of the YAG:Ce powder increased with the annealing temperature. Moreover, it is clearly seen that, for the sample annealed at 1000°C, there are many smaller particles which are attached to the surface of a number of large particles (Figure 5(b)). This phenomenon was observed also for the sample annealed at low temperature (Figure 5(a)) but not observed for the high annealing temperature sample (Figure 5(c)). Indeed, the size of such small particles can be evaluated on the FE-SEM micrographs, and it is from approximately 10 nm to 20 nm. With the calcination temperature increased to 1200°C, the grain size grew to a few micrometers (1–3 μ m).

The DLS measurement results for the particle size distribution from the WDT-dispersed solution are shown in Figure 6(a). The particle distribution shown in this figure indicates that, for the sample annealed at 700°C, particles have a size ranging from 0.2 to 3.3 μ m; among them, a large number of particles are 0.5 μ m and 3.2 μ m in size (see two peaks in "1" of Figure 6(a)). For the samples annealed at 1000°C and 1200°C, larger particles are observed and their size is in the range from 0.6 to 3.3 μ m and 1.0 to 3.3 μ m, respectively (see "2" and "3" in Figure 6(a)). This indicates that for the YAG:Ce synthesis, the annealing temperature strongly affected the growth of the particle size. The particle size of YAG:Ce annealed at 1200°C is much larger in comparison with samples annealed at 700 and 1000°C. The smallest particle size is about 1 μ m. These particle size distribution pictures do not reflect what was observed in the SEM micrographs: from the particle size distribution curves no nanoparticles were observed. This means that by the WDT

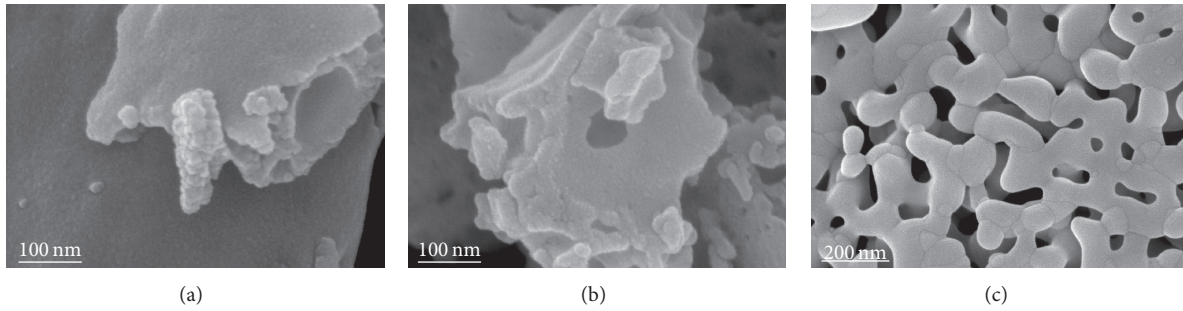


FIGURE 5: FE-SEM images of YAG:Ce powders annealed for 5 h at 700°C (a), 1000°C (b), and 1200°C (c).

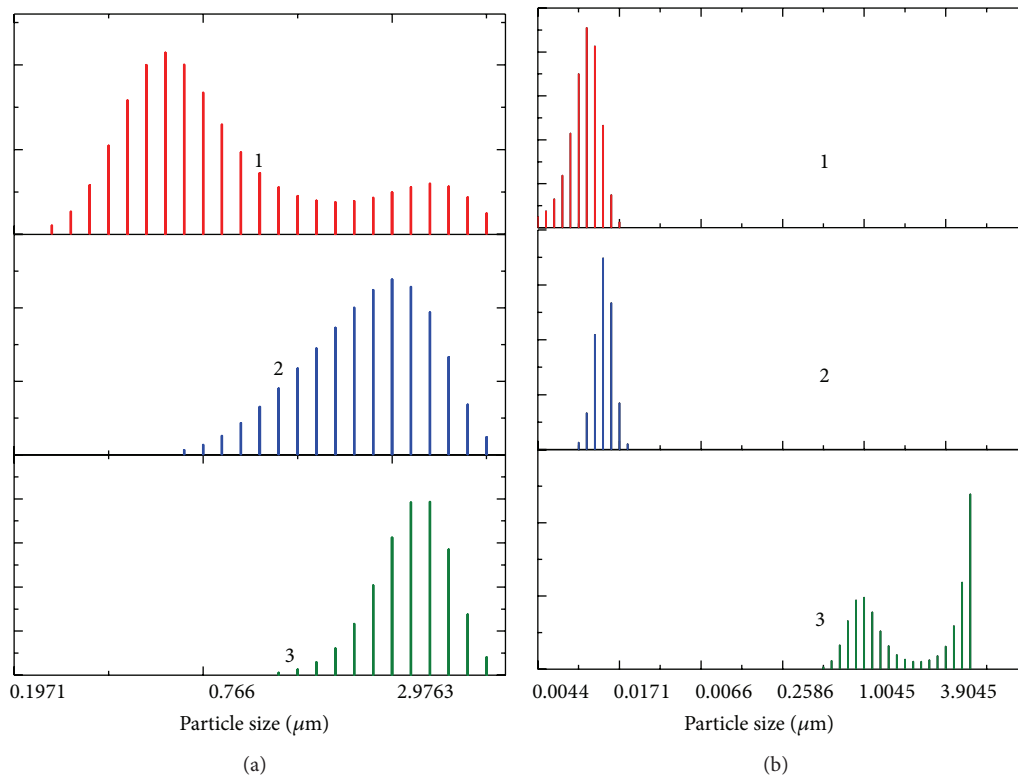


FIGURE 6: Particle size distribution obtained by DLS method for YAG:Ce dispersed solutions for the samples annealed at 700°C (1), 1000°C (2), and 1200°C (3) using WDT (a) and NST (b) techniques for the dispersion.

method it is impossible to completely disperse (or separate) the nanoparticles from the large particles.

The measurement results of the particle size distribution from the NST dispersed solution are plotted in Figure 6(b). From this figure, one can see that almost all particles in the solution obtained from the sample annealed at 700°C are nanocrystalline. Their size varies from 4 to 17 nm. Whereas for the sample annealed at 1000°C, the dispersed particles have a size ranging from 8.7 nm to 20 nm, and for the sample annealed at 1200°C, there are no observed nanoparticles in the NST dispersion solution.

From the results obtained on the YAG:Ce powder dispersion, one can note that the YAG:Ce nanoparticles formed

during the LTC synthesis were completely dispersed due to the NST method, whereas by the WDT method only a small part of the nanoparticles can be separated from the microclusters. This is in agreement with what was observed in the SEM micrographs.

The photoluminescence of the solution containing the YAG-Ce nanoparticles was also investigated. Indeed, the nanoparticle effect on the PL was observed when the dispersion solution was used as a target for photoluminescence measurements. In Figure 7, two PL curves are shown corresponding to two solutions with the NST treatment durations of 30 min and 60 min, respectively. The powder used for the NST treatment was taken from a YAG:Ce

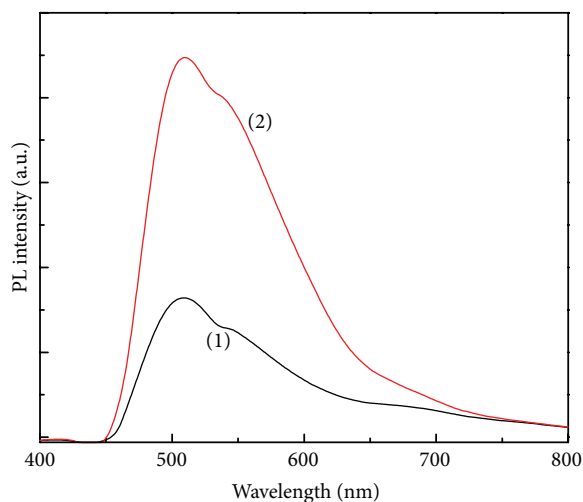


FIGURE 7: Photoluminescence of nano-YAG:Ce particles solutions with the NST treatment of 30 min (1) and 60 min (2) at 442 nm excited wavelength.

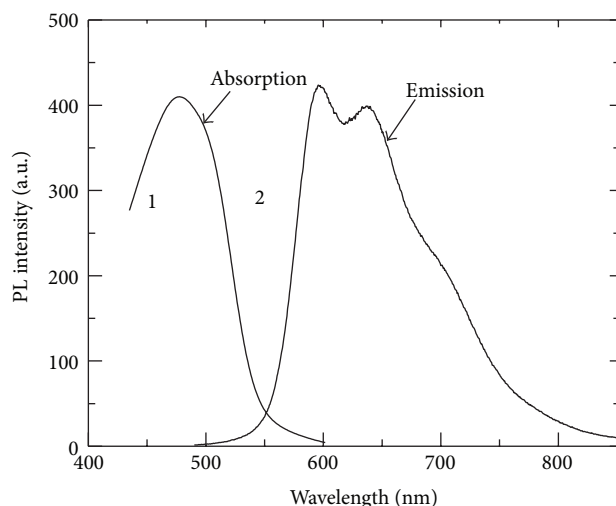


FIGURE 8: Absorption (1) and emission (2) spectra of the MEH-PPV film. The thickness $d = 200$ nm.

sample annealed at 1000°C . The excitation wavelength used for the PL measurements was 442 nm. Compared with the PL of the YAG:Ce powder (see Figure 4), the PL curves of nano-YAG:Ce particles solution have a similar shape. The spectra are also broad, expanding from 470 nm to 750 nm. The fact that the PL intensity increased with the increase of the treatment time proved that the dispersion solution became much enriched with YAG:Ce nanoparticles. The peak of both the two PL spectra was found to be of ca. 510 nm. This value is slightly (10 nm) smaller than the PL peak wavelength value (520 nm) of the PL spectra for the YAG:Ce powder (see Figure 4). This blue shift can be explained by the nanosize effect in the PL emission for the semiconducting nanoparticles and/or quantum dots [20, 21].

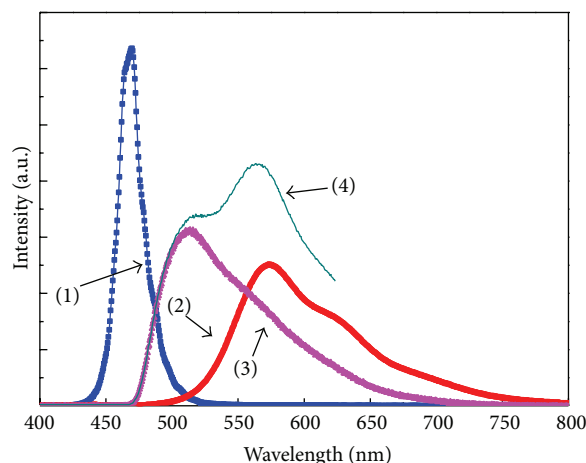


FIGURE 9: Emission spectra of components of WLEDs made from nanocomposite: blue LED (curve 1), MEH-PPV (curve 2), YAG:Ce nanopowder (curve 3), and the total spectrum of the blue LED, nanocomposite “YAG:Ce + MEH-PPV” (curve 4).

3.3. Spectra of WLED. The absorption and photoluminescence spectra of MEH-PPV film were plotted in Figure 8. From this figure one can see that the MEH-PPV film has an absorption peak at 480 nm and two emission peaks at 570 nm and 640 nm. This is consistent with the reporting results on MEH-PPV films deposited by spin coating for preparation of OLED [22]. Thus, a blue LED chip can be used for exciting luminescence of the MEH-PPV.

In Figure 9, the electroluminescence spectra of a blue LED, photoluminescence spectra of YAG:Ce, and MEH-PPV polymer are presented. From this figure one can expect that the light emitted from three components as the blue LED chip, YAG:Ce green phosphor, and MEH-PPV yellow polymer could exhibit the white light with a broad band luminescent spectrum and a high color rendering index (CRI). Especially, with the use of YAG:Ce + MEH-PPV hybrid composite, the spectral region is enhanced around the wavelength of 521 nm. This is due to the contribution of the emission of the nano-YAG:Ce phosphor. The increase of the intensity of the 521 nm peak enables the CRI increase. In addition, similar to the other quantum dots like CdSe, ZnSe, and so forth, the nano YAG:Ce particles possessing such a strong PL property can be used for biomarkers, pigments in printing, and organic and inorganic hybrid solar cells.

4. Conclusion

The nano-YAG:Ce powder was prepared by a sol-gel low temperature combustion method, followed by thermal annealing. The optimal annealing temperature of the sample used for enriching nanoparticles solution by using the NST method was found to be of 1000°C . By NST treatments, uniform YAG:Ce nanoparticles of 9–20 nm have been collected and mixed with MEH-PPV conjugated polymer to get nanocomposites. WLEDs made from the blue LED chip coated with the nano-YAG:Ce + MEH-PPV composite epoxy exhibit white

light with a broad band luminescent spectrum and a high color rendering index (CRI).

The photoluminescence spectra of the YAG:Ce nanoparticles showed a potential application of the prepared nanostructured YAG:Ce phosphor not only in energy-efficient solid-state lighting, but also in optoelectronic devices, including organic composite solar cells.

Conflict of Interests

The authors declare that there is no conflict of interests regarding the publication of this paper.

Acknowledgments

This research is funded by Vietnam National Foundation for Science and Technology (NAFOSTED) under Grant no. “103.02-2013.39.” Infrastructure and equipment provided for YAG:Ce synthesis, XRD patterns, and NST treatments were made possible in the VNU project on “Nanotechnology and Application” in the period 2010–2013 supported by the Vietnamese Government.

References

- [1] S. Nakamura, T. Mukai, and M. Senoh, “Candela-class high-brightness InGaN/AlGaIn double-heterostructure blue-light-emitting diodes,” *Applied Physics Letters*, vol. 64, no. 13, pp. 1687–1689, 1994.
- [2] M. Yamada, T. Mitani, Y. Narukawa et al., “InGaIn based near-ultraviolet and blue-light-emitting diodes with high external quantum efficiency using a patterned sapphire substrate and a mesh electrode,” *Japanese Journal of Applied Physics*, vol. 41, pp. L1431–L1433, 2002.
- [3] N.-C. Chen, C.-M. Lin, Y.-K. Yang, C. Shen, T.-W. Wang, and M.-C. Wu, “Measurement of junction temperature in a nitride light-emitting diode,” *Japanese Journal of Applied Physics*, vol. 47, no. 12, pp. 8779–8782, 2008.
- [4] S. Muthu, F. J. P. Schuurmans, and M. D. Pashley, “Red, green, and blue LEDs for white light illumination,” *IEEE Journal on Selected Topics in Quantum Electronics*, vol. 8, no. 2, pp. 333–338, 2002.
- [5] Y. Shimizu, “Development of White LED light source,” *Rare Earth*, vol. 40, pp. 150–151, 2002.
- [6] H. S. Jang and D. Y. Jeon, “Yellow-emitting $\text{Sr}_3\text{SiO}_5:\text{Ce}^{3+}, \text{Li}^+$ phosphor for white-light-emitting diodes and yellow-light-emitting diodes,” *Applied Physics Letters*, vol. 90, no. 4, Article ID 041906, 2007.
- [7] Y. X. Pan, M. M. Wu, and Q. Su, “Tailored photoluminescence of YAG:Ce phosphor through various methods,” *Journal of Physics and Chemistry of Solids*, vol. 65, pp. 845–850, 2004.
- [8] J.-G. Li, T. Ikegami, J.-H. Lee, T. Mori, and Y. Yajima, “Co-precipitation synthesis and sintering of yttrium aluminum garnet (YAG) powders: the effect of precipitant,” *Journal of the European Ceramic Society*, vol. 20, no. 14–15, pp. 2395–2405, 2000.
- [9] J. S. Abell, I. R. Harris, B. Cockayne, and B. Lent, “An investigation of phase stability in the $\text{Y}_2\text{O}_3\text{-Al}_2\text{O}_3$ system,” *Journal of Materials Science*, vol. 9, no. 4, pp. 527–537, 1974.
- [10] Q. Zhang and F. Saito, “Mechanochemical solid reaction of yttrium oxide with alumina leading to the synthesis of yttrium aluminum garnet,” *Powder Technology*, vol. 129, no. 1–3, pp. 86–91, 2003.
- [11] J. Su, Q. L. Zhang, C. J. Gu et al., “Preparation and characterization of $\text{Y}_3\text{Al}_5\text{O}_{12}$ (YAG) nano-powder by co-precipitation method,” *Materials Research Bulletin*, vol. 40, no. 8, pp. 1279–1285, 2005.
- [12] Z. H. Wang, L. Gao, and K. Niihara, “Synthesis of nanoscale yttrium aluminium garnet powder by the co-precipitation method,” *Materials Science and Engineering*, vol. A288, pp. 1–4, 2000.
- [13] C. J. Liu, R. M. Yu, Z. W. Xu, J. Cai, X. H. Yan, and X. T. Luo, “Crystallization, morphology and luminescent properties of YAG:Ce³⁺ phosphor powder prepared by polyacrylamide gel method,” *Transactions of Nonferrous Metals Society of China*, vol. 17, no. 5, pp. 1093–1099, 2007.
- [14] M. Veith, S. Mathur, A. Kareiva, M. Jilavi, M. Zimmer, and V. Huch, “Low temperature synthesis of nanocrystalline $\text{Y}_3\text{Al}_5\text{O}_{12}$ (YAG) and Ce-doped $\text{Y}_3\text{Al}_5\text{O}_{12}$ via different sol-gel methods,” *Journal of Materials Chemistry*, vol. 9, no. 12, pp. 3069–3079, 1999.
- [15] X. H. Yan, S. S. Zheng, R. M. Yu et al., “Preparation of YAG:Ce³⁺ phosphor by sol-gel low temperature combustion method and its luminescent properties,” *Transactions of Nonferrous Metals Society of China*, vol. 18, no. 3, pp. 648–653, 2008.
- [16] S. K. Brar and M. Verma, “Measurement of nanoparticles by light-scattering techniques,” *Trends in Analytical Chemistry*, vol. 30, no. 1, pp. 4–17, 2011.
- [17] D. N. Chung, N. N. Dinh, D. N. Hieu, and P. H. Duong, “Synthesis of cerium-doped yttrium aluminum garnet nanopowder low-temperature reaction combustion method,” *VNU Journal of Science, Mathematics—Physics*, vol. 2, pp. 53–60, 2013.
- [18] W. B. Russel, “Brownian motion of small particles suspended in liquids,” *Annual Review of Fluid Mechanics*, vol. 13, pp. 425–455, 1981.
- [19] B. D. Cullity, *Elements of X-Ray Diffraction*, Addison, Wesley Publishing Company, Reading, Mass, USA, 2nd edition, 1978.
- [20] U. Woggon, *Optical Properties of Semiconductor Quantum Dots*, vol. 136 of *Springer Tract in Modern Physics*, Springer, Berlin, Germany, 2013.
- [21] A. Wolcott, D. Gerion, M. Visconte et al., “Silica-coated CdTe quantum dots functionalized with thiols for bioconjugation to IgG proteins,” *Journal of Physical Chemistry B*, vol. 110, no. 11, pp. 5779–5789, 2006.
- [22] N. N. Dinh, L. H. Chi, T. T. Chung Thuy, T. Q. Trung, and V.-V. Truong, “Enhancement of current-voltage characteristics of multilayer organic light emitting diodes by using nanostructured composite films,” *Journal of Applied Physics*, vol. 105, no. 9, Article ID 093518, 5 pages, 2009.



Hindawi

Submit your manuscripts at
<http://www.hindawi.com>

